Slingo, Mary and Cole, Mark and Carr, Carolyn and Curtis, Mary K. and Dodd, Michael and Giles, Lucia and Heather, Lisa C. and Tyler, Damian and Clarke, Kieran and Robbins, Peter A. (2016) The von Hippel-Lindau Chuvash mutation in mice alters cardiac substrate and high energy phosphate metabolism. American Journal of Physiology – Heart and Circulatory Physiology . ISSN 1522-1539

Title page

The von Hippel-Lindau Chuvash mutation in mice alters cardiac substrate and high energy phosphate metabolism

Mary Slingo, Mark Cole, Carolyn Carr, Mary K. Curtis, Michael Dodd, Lucia Giles, Lisa C Heather, Damian Tyler, Kieran Clarke, Peter A Robbins.

All affiliations:
Department of Physiology, Anatomy and Genetics. University of Oxford,
Sherrington Building,
Parks Road,
Oxford,
OX1 3PT
UK.

MS – designed and performed study, performed data analysis, wrote the manuscript.
MC – designed and performed study, performed data analysis.
CC – performed *in vivo* cine MRI and assisted with analysis.
KC – performed gene analysis and assisted with analysis.
MD and LG – performed hyperpolarized MRI study and its analysis.
LH – assisted with design of study, radiolabelled substrate perfusion, and assisted with analysis.
DT – assisted with cine MRI and hyperpolarized MRI and data analysis.
KC and PR – designed study, assisted with data analysis, reviewed the manuscript.

Corresponding author for production only:
Dr Mary Slingo
+44 7900 953919
maryslingo@doctors.org.uk

Corresponding author upon publication:
Prof Peter A Robbins
Peter.robbins@dpag.ox.ac.uk. Tel: +44 (0)1865 272490.

Abstract

Hypoxia-inducible factor (HIF) appears to function as a global master regulator of cellular and systemic responses to hypoxia. HIF-pathway manipulation is of therapeutic interest, however global, systemic upregulation of HIF may have as yet unknown effects on multiple processes. We utilized a mouse model of Chuvash polycythemia (CP), a rare genetic disorder which modestly increases expression of HIF target genes in normoxia, to understand what these effects might be within the heart.

An integrated *in* and *ex vivo* approach was employed. In comparison to wild-type controls, CP mice had evidence (using *in vivo* MRI) of pulmonary hypertension, right ventricular hypertrophy, and increased left ventricular ejection fraction. Glycolytic flux (measured using ^{3}H glucose) in the isolated, contracting, perfused CP heart was 1.8-fold higher. Net lactate efflux was 1.5-fold higher. Furthermore, *in vivo* ^{13}C magnetic resonance spectroscopy (MRS) of hyperpolarized $^{13}C_1$ pyruvate revealed a 2-fold increase in real-time flux through lactate dehydrogenase in the CP hearts, and a 1.6-fold increase through pyruvate dehydrogenase. ^{31}P MRS of perfused CP hearts under increased workload (isoproterenol infusion) demonstrated increased depletion of phosphocreatine relative to ATP. Intriguingly, no changes in cardiac gene expression were detected.

In summary, a modest systemic dysregulation of the HIF pathway resulted in clear alterations in cardiac metabolism and energetics. However, in contrast to studies generating high HIF levels within the heart, the CP mice showed neither the predicted changes in gene expression nor any degree of LV impairment. We conclude that the effects of manipulating HIF on the heart are dose-dependent.

New and noteworthy

This is the first integrative metabolic and functional study of the effects of modest HIF manipulation within the heart. Of particular note, the combination (and correlation) of perfused heart metabolic flux measurements with the new technique of real-time *in vivo* MR spectroscopy using hyperpolarized pyruvate is a novel development.

Keywords

Hypoxia-inducible factor, cardiac metabolism, MRI, hyperpolarized pyruvate, Chuvash polycythemia

Introduction

Prolonged hypoxia results in diverse changes within multiple organ systems - ventilatory acclimatization, increased erythropoiesis, pulmonary vascular remodeling, and metabolic alterations occur(54). Many of these diverse cellular and systemic responses to hypoxia are, or are likely to be, coordinated by the hypoxia-inducible factor (HIF) family of transcription factors. HIF is a heterodimer, comprising an oxygen-regulated alpha subunit (HIF-1α, HIF-2α, or HIF-3α) and a ubiquitous beta subunit (HIF-1β). The stability of HIF-α subunits is regulated by oxygen-dependent prolyl hydroxylation (by prolyl-4-hydroxylase domain proteins, PHDs) which enables recognition by the von Hippel-Lindau (VHL) ubiquitin E3 ligase and subsequent degradation via the ubiquitin-proteasome pathway(31, 54). Hence, HIF appears to function as a global master regulator of cellular and systemic responses to hypoxia in all metazoan species studied to date(36).

There is considerable interest in understanding further the role of HIF in both individual organ systems and within integrative physiology, driven in part by the potential benefits of VHL-HIF pathway manipulation in the treatment of cancer and vascular disease(49). For example, global, systemic upregulation of HIF may have as yet unknown effects on multiple cellular and physiological processes. We sought to understand what these effects might be within the heart.

Exposure of animals and humans to sustained hypoxia results in a consistent pattern of myocardial alterations in metabolic gene expression, substrate utilization, energetics, and function. The dynamic changes in gene expression increase the capacity for glucose uptake(63) and utilization(1, 62), whilst capacity for fatty acid utilization is reduced(62). Indeed, myocardial glucose uptake is increased in high-altitude natives(21) and in rats exposed to hypobaric hypoxia(28). These alterations in substrate utilization may affect myocardial energetics and function – lower phosphocreatine (PCr):ATP ratios were observed in Sherpa hearts(20), in lowlanders exposed to 20 hours of normobaric hypoxia (with accompanying diastolic dysfunction)(22), and in trekkers travelling to Everest base camp at 5300 m (also with impaired diastolic function)(23).

It is of note that the cardiac metabolic changes seen in response to hypoxia are similar to those observed in heart failure(34, 43-45). Indeed, it has been hypothesized that

myocardial hypoxia, with consequent activation of the HIF pathway, may play a role in altering cardiac substrate utilization, energetics and contractile function; these changes may then cause or exacerbate heart failure. This hypothesis has been explored in experiments producing very high levels of HIF in the heart, from which it is clear that major alterations in HIF give rise to metabolic changes and cardiomyopathy(7, 24, 29, 35, 40, 41). However, these experiments do not reveal whether more modest alterations in HIF, particularly at a systemic level, produce similar results.

Chuvash polycythemia (CP) is a rare autosomal recessive disorder with the potential to address this question. CP arises from a single point mutation in *VHL* which diminishes the binding affinity of the protein for hydroxylated HIF-1α and HIF-2α, increasing the expression of HIF target genes under normoxic conditions(2, 14). Patients with CP develop polycythemia, pulmonary hypertension, increased ventilatory and pulmonary vascular sensitivity to hypoxia, and altered skeletal muscle metabolism and energetics(14, 65), although any effects on cardiac function remain unidentified. Many aspects of the human disease have been shown to be faithfully recapitulated in the mouse model(18, 19, 39, 64).

The CP mouse therefore provides a unique opportunity to study the effects on the heart of long term, systemic activation of the HIF pathway at more 'physiological' levels, without the confounding influence of periods of reduced oxygen availability through hypoxia. The purpose of the present study was to investigate the cardiac metabolic and functional phenotype of CP, utilizing both *in*- and *ex-vivo* techniques.

Methods

Animals. CP breeding pairs were donated, and the original mutation was generated on a C57BL6 background as described previously(18). CP and wild type (homozygous, WT) mice (from the same breeding colony of mice heterozygous for the *VHL* Chuvash mutation) were used for all comparisons. All animal procedures were compliant with both the UK Home Office Animals (Scientific Procedures) Act 1986 and the Local Ethical Review Procedures (University of Oxford Medical Sciences Division Ethical Review Committee). Mice were housed within individually ventilated cages, in room air, with free access to food and water.

Hematology and analysis of plasma metabolites. Following excision of the heart for perfusion, blood was collected immediately from the chest cavity. Hematocrits, in a heparinized capillary tube, were measured using a hematocrit centrifuge (Hettich, Germany); hemoglobin was measured using a HemoCue Hb 201+ (HemoCue, UK). The remaining blood was centrifuged at 4 °C and the plasma subsequently frozen in liquid nitrogen. All plasma analysis was performed on an ABX Pentra 400 Clinical Chemistry analyzer (Horiba ANX S.A.S, UK).

Cardiac magnetic resonance imaging (MRI). Anesthesia was induced using 5%, and maintained with 1 – 2%, isoflurane in 100% O_2. Respiratory rate and ECG were monitored continuously. Cine MRI was performed as described previously(58). Mice were placed in a purpose-built cradle, which was lowered into a vertical-bore 11.7 T (500 MHz) system (Magnex, UK) with a 40 mm birdcage coil (Bruker, Germany). A stack of contiguous, 1 mm thick, true short axis ECG- and respiration-gated cine/FLASH images were acquired to cover the entire heart. Image data were analyzed using the ImageJ software (NIH Image, USA). End-systole (ES) and end-diastole (ED) frames for each slice were identified and the LV endo- and epi-cardial borders outlined in all slices to give values for ESV (end-systolic volume) and EDV. Stroke volume (SV = EDV – ESV), ejection fraction (EF = (SV/EDV) x 100), and cardiac output (CO = SV x heart rate) were calculated. LV mass was calculated as the product of the LV volume and the specific gravity of myocardium (1.05 g/cm^3). The mid-ventricular (MV) slice was defined as the one in which the papillary muscles were most prominent; right ventricle (RV) free wall thickness was measured in three separate locations in this slice, and subsequently averaged.

To quantify septal bowing (the distortion of the LV), a novel method was used. First, the LV epi-cardial border in early-diastole in the MV slice was outlined, giving an actual perimeter length (P_A) and area (A_A). The maximum possible area enclosed by a perimeter of any given length arises when the figure is a circle. For a perimeter of length P_A, we denote this area as A_C. If the LV were perfectly circular, then the ratio of A_A to A_C would be 1. As the LV becomes increasingly distorted in shape A_A falls relative to A_C, and hence the ratio will fall below 1. This 'septal bowing ratio' thus enables quantification of the distortion of the septum using the LV itself as the comparator. We chose to quantify septal bowing in this way, as it is an approach that is likely to be relatively insensitive to observer variability. We expect that a relatively linear relationship would exist between this index and other indices of septal bowing, such as the ratio between the long and short axes in a short-axis ventricular slice (as introduced by Ryan et al.(56), and which correlates with pulmonary artery pressure in patients with pulmonary hypertension), but this has not been tested directly.

Gene expression (Real-Time PCR). Total RNA was extracted from 20 – 30 mg powdered (in liquid nitrogen) whole-heart tissue (following Langendorff perfusion) and whole-lung tissue. Total RNA was extracted using the Rneasy Fibrous Kit (Qiagen, UK), including a Dnase treatment step, and complementary DNA immediately synthesized from 1 μg RNA using the Applied Biosystems High Capacity cDNA Reverse Transcription Kit (Life Technologies, UK). Real-Time PCR was performed using an ABI Prism 7000 Sequence Detection System (Applied Biosystems, UK) with TaqMan Universal PCR Master Mix and TaqMan Gene Expression Assays (choosing manufacturer-recommended assays: Applied Biosystems, UK). Relative quantification of mRNA expression levels was determined using the standard curve method and normalized to beta-actin (heart tissue) or 18s ribosomal RNA (lung tissue).

Gene expression (Micro-array). Total RNA was extracted from 20 – 30 mg powdered (in liquid nitrogen) whole-heart tissue using the Rneasy Fibrous Kit (Qiagen, UK), including a Dnase treatment step. The RNA integrity was assessed on a BioAnalyzer (Agilent Laboratories, US); all samples had a RNA Integrity Number (RIN) ≥ 7. Labelled sense ssDNA for hybridisation was generated from 200 ng starting RNA with the Ambion WT expression kit (P/N 4411973) and the Affymetrix GeneChip WT Terminal Labeling and Controls Kit (P/N 901525) according to the manufacturer's instructions. The distribution of fragmented sense ssDNA lengths was measured on the BioAnalyser. The fragmented ssDNA was labeled and hybridised for 17 hours at 45 °C to the Affymetrix

GeneChip Human Mouse 1.0 ST Array (Affymetrix). Chips were processed on an Affymetrix GeneChip Fluidics Station 450 and Scanner 3000. Affymetrix Command Console was used to generate cel files and Affymetrix Expression Console was used for the quality control. Arrays were RMA normalised in GeneSpring GX 12 and differentially expressed genes were identified using Limma with a Benjamini and Hochberg multiple testing correction of ≤ 0.05. As few genes were detected using this method the data were re-analysed using PLIER normalisation and a Student's t-test with a p-value cut off of ≤ 0.05 and a fold change difference between wild type and Chuvash of ≥ 1.3.

Isolated heart perfusion. Mice were terminally anesthetized with an intraperitoneal injection of sodium pentobarbitol (500 mg/kg, Merial, UK) and the heart excised and arrested in ice-cold Krebs-Henseleit buffer; blood was immediately collected from the chest cavity for subsequent analysis. The ascending aorta was cannulated and the heart perfused retrograde in Langendorff mode at 37 °C at a constant perfusion pressure of 80 mmHg. A polyethylene balloon, connected to a pressure transducer and used to measure cardiac function, was inserted into the left ventricle (LV) lumen and its volume adjusted to produce an end-diastolic pressure (EDP) of 4 – 8 mmHg. Rate pressure product (RPP) was calculated as the product of LV developed pressure (systolic pressure minus EDP) and heart rate. Hearts were perfused with 100 ml of a modified Krebs-Henseleit re-circulating buffer (118 mmol/L NaCl, 3.7 mmol/L KCl, 1.2 mmol/L $MgSO_4$, 1.97 mmol/L $CaCl_2$, 0.5 mmol/L Na_2EDTA, 25 mmol/L $NaHCO_3$, 1.2 mmol/L KH_2PO_4) containing 11 mmol/L glucose and 0.4 mmol/L palmitate pre-bound to 1.5 % albumin as substrates. The buffer was continually gassed with a mix of 95% O_2 with 5 % CO_2.

Perfused heart energetics. Perfused hearts were inserted into an 11.7 T (500 MHz) vertical bore (123 mm internal diameter) magnet (Magnex Scientific, UK) with a 10 mm probe (Rapid, Germany) containing concentric ^{1}H and ^{31}P sensitive coils. Fully relaxed ^{31}P spectra were acquired using pulse-and-collect sequence at a repetition time of 10 s and a flip angle of 90° (32 averages, total acquisition time of 5 min, steady state. Approximate doubling of the RPP was then achieved by an infusion of isoproterenol (concentration received by the heart 2 – 5 nM) and further spectra acquired (minimum acquisition time 5 min). Spectra were analyzed using the jMRUI software(42) to give values for phosphocreatine (PCr) and γATP abundance, and the ratio of these two. Spectra for each perfusion condition (standard, or isoproterenol) were averaged to give final values for PCr:ATP.

Measurement of cardiac substrate metabolism. To determine glycolytic flux in the perfused heart, 50 μCi of D[5-^{3}H]-glucose (Amersham, UK) were added to the re-circulating buffer. Following a 10 min stabilization period, perfusate samples were collected at 5 min intervals for 35 min. $^{3}H_20$ was separated from the D[5-^{3}H]-glucose in the time samples using Dowex® ion exchange resin (Sigma, UK) and subsequently used to calculate the glycolytic rate. Due to the position of the ^{3}H label, this method gives a measure of true glycolytic rate since the label is cleaved by enolase in the cytosol.

Cardiac lactate efflux was determined by measuring lactate concentration spectrophotometrically in timed perfusate collections using lactate dehydrogenase. This method gives a measure of net lactate efflux from the heart. Cardiac palmitate oxidation rates were determined in a separate group of perfused hearts by adding 50 μCi of [9,10-^{3}H]-palmitate (Amersham, UK) to the re-circulating buffer and performing a chloroform-methanol Folch extraction on the time buffer samples to collect the $^{3}H_20$.

Measurement of in vivo cardiac metabolism in real-time. Mice were studied in the early absorptive (fed) state, between 1 and 11 am. They were anesthetized in isoflurane and O_2 and intravenous access was gained using a 32 G tail-vein cannula. Mice were then positioned within a 7 T horizontal-bore MR scanner. Respiratory rate and ECG were monitored continuously. As described previously(12), 0.15 ml of hyperpolarized $^{13}C_1$ pyruvate (0.48 mmol/kg) was injected over 10 s, followed by a 0.05 ml flush of heparinized saline to clear the delivery line. Sixty individual ECG-gated ^{13}C MR cardiac spectra were acquired over 1 min following injection and subsequently analyzed using the AMARES algorithm in the jMRUI software package (Version 4.0(42)). The peak areas of $^{13}C_1$ pyruvate, $^{13}C_1$ lactate, $^{13}C_1$ alanine and $^{13}C_1$ bicarbonate at each time point were quantified and used as input data for a kinetic model as described previously(12).

Statistical analysis. Differences between groups were assessed using one-way analysis of variance using SPSS Statistics 19 (IBM, USA).

Results

The purpose of this study was to determine the cardiac metabolic and functional phenotype of the CP mouse, in comparison with the WT.

General hematological and biochemical characteristics of the CP mouse model. Body mass, basic hematology and plasma metabolites are summarized in Table 1. Polycythemia in the CP mice was confirmed by demonstrating a modest increase in both hemoglobin and hematocrit, consistent with previous reports(18, 19, 64). No differences were seen in non-fasting plasma metabolites.

CP mice have normal cardiac metabolic gene expression. The whole-heart expression of key cardiac metabolic genes revealed no differences between WT and CP mice (Figure 1). In order to confirm the methodology, the expression of lung endothelin-1 was studied and found to be significantly increased in the CP mice, in keeping with previous findings(19). The full micro-array results are included in the supplemental material.

CP mice exhibit features of pulmonary hypertension. Cardiac function and mass in WT and CP mice at different ages are shown in Figure 2. A full table of cine MRI results is included in Table 2.

RV free wall hypertrophy, a typical feature of pulmonary hypertension, was seen in all age groups in the CP mice (Figure 2B). These findings were comparable with those reported in a previous study, in which pulmonary artery pressure and RV free wall thickness were measured using invasive techniques (19). In addition, marked interventricular septal bowing, another characteristic feature of pulmonary hypertension, was seen in all age groups in the CP mice (Figure 2F). The degree of septal bowing was quantified and is included in Table 2.

In contrast to the marked changes in the RV, no differences were seen in LV mass or cardiac output (corrected for body mass; Figures 2A and C). Interestingly, LV ejection fraction was significantly increased in the younger CP mice, perhaps as a result of the pulmonary hypertension (Figure 2D).

CP hearts exhibit more marked depletion of phosphocreatine under conditions of high workload. ^{31}P MR spectroscopy of Langendorff-perfused hearts enabled the measurement of cardiac energetics under conditions of both normal and high workload.

Although cardiac energetics were similar in WT and CP hearts perfused under normal conditions, an infusion of isoproterenol (causing an approximate doubling in RPP) resulted in significantly lower PCr:ATP ratios in the CP hearts compared with WT controls (PCr:ATP 1.21 ± 0.08 in CP versus 1.56 ± 0.08, $p < 0.02$) (Figure 3).

Glycolytic flux and lactate efflux are increased in the CP heart. Glycolytic flux in the perfused heart, measured using ^{3}H-glucose, was 1.8-fold higher in the CP heart compared with WT controls (Figure 4A). Analysis of variance, using genotype (CP or WT) as the fixed factor and heart mass and RPP as co-variates, demonstrated that the CP mutation was the only significant determining factor on glycolytic rate ($p = 0.004$ for genotype; $p = 0.095$ for heart weight; $p = 0.147$ for RPP). Similarly, net lactate efflux was 1.5-fold higher in the CP hearts ($p = 0.009$ for genotype; $p = 0.121$ for heart weight; $p = 0.123$ for RPP) (Figure 4B). There was a significant correlation between glycolytic and lactate efflux rates (Pearson R = 0.935, $p < 0.0001$). In contrast to the increased glucose utilization and lactate production by the CP hearts, a decrease in fatty acid oxidation (as might be predicted by the Randle Cycle(27)) was undetectable (Figure 4C).

In vivo pyruvate metabolism, measured in real-time, is significantly altered in the CP heart. The advent of dynamic nuclear polarization (DNP) has enabled the study of cardiac metabolism in real-time(59). *In vivo* ^{13}C MR spectroscopy of hyperpolarized $^{13}C_1$ pyruvate revealed, in keeping with the perfusion studies, a 2-fold increase in the rate of $^{13}C_1$ label incorporation into lactate in the CP hearts ($p < 0.01$, Figure 5). Furthermore, there was a 1.6-fold increase in the rate of label incorporation into bicarbonate ($p < 0.05$), indicating elevated flux through pyruvate dehydrogenase (Figure 5).

Discussion

It is now known that HIF functions as a global master regulator, coordinating diverse cellular and systemic responses to hypoxia. Studies on patients and mice have demonstrated that perturbations in the HIF pathway, such as Chuvash polycythemia or HIF-2α gain-of-function mutations, result in profound abnormalities in systemic and cellular processes that are usually under tight control. Marked changes in skeletal muscle metabolism, ventilation, pulmonary vascular tone, and glucose homeostasis are all observed in both humans and animals with disorders of the HIF pathway(2, 13-16, 18, 19, 37, 39, 46, 48, 50-53, 57, 64-66, 68, 69). We now demonstrate that chronic, modest upregulation of HIF due to the Chuvash *VHL* mutation results in altered cardiac metabolism and energetics in the mouse heart.

A primordial function of HIF-1 is to find the optimal balance between oxidative and glycolytic metabolism for a given local oxygen concentration. As such, HIF-1 target genes, including glucose transporters and glycolytic enzymes(30, 60), lactate dehydrogenase (LDH)(61) and pyruvate dehydrogenase kinase 1 (PDK-1)(33, 47), enable increased glucose metabolism. In both hypoxia and hypoxia-mimetic models, myocardial expression of the master regulator of fatty acid metabolism, peroxisome proliferator-activated receptor α (PPARα), is decreased together with its downstream targets such as PDK-4(1, 55, 62). Alterations in cardiac mitochondrial oxidative metabolism are also seen(17). Thus, one would predict that exposure to hypoxia, or chronic activation of the HIF pathway, would result in an increased reliance upon glycolysis and glucose oxidation, and a shift away from fatty acid beta-oxidation.

Most studies investigating the role of HIF in cardiac metabolism and function have employed tactics either to over-express HIF itself, or to impair its degradation by using altered levels of PHDs or VHL. Mice with cardiomyocyte-specific loss of VHL have elevated HIF levels in the heart, accompanied by increased expression of glycolytic genes, cellular lipid accumulation, and progressive heart failure(35). Combined cardiac-specific loss of both PHD2 and PHD3 results in increased expression of phosphoglycerate kinase (PGK), decreased expression of PPARα, myocyte accumulation of lipid, and severe cardiomyopathy(41). Conditional somatic inactivation of PHDs produces similar results(40). Inducible cardiac-specific overexpression of an oxygen-stable form of HIF-1α results in increased transcript levels of glycolytic genes and progressively impaired cardiac function(7). Furthermore, long-term constitutive

overexpression of HIF-1α results in increased glucose uptake and the development of cardiomyopathy(24). Taken together, these studies have shown that very high levels of HIF in the heart result in a switch in gene expression towards increased glucose metabolism, with accompanying contractile dysfunction. In contrast, shorter-term constitutive overexpression of HIF-1α mRNA in cardiomyocytes did not result in cardiomyopathy, but this construct only produced a barely detectable increase in HIF in normoxia. Interestingly, this overexpression was protective during myocardial infarction, where hypoxia would be expected to be present (32).

Our study investigated the cardiac effects of the Chuvash *VHL* mutation in mice, which results in systemic, long-term, modest upregulation of HIF. Our model faithfully recapitulated findings seen in previous studies on CP patients and mice – raised hemoglobin and hematocrit, pulmonary hypertension (shown using non-invasive MRI), and RV hypertrophy (using MRI, rather than histology). However, a surprising feature of our study was the apparent lack of change in the expression of key metabolic genes within the heart, despite clear alterations in substrate metabolism and energetics. It is possible that our whole-heart analysis masked differential changes that could have been seen in the left, versus the right, ventricle(1, 62). Alternatively, the presence of pulmonary hypertension and right ventricular hypertrophy may have resulted in genetic remodeling in addition to that caused by the Chuvash *VHL* mutation. Finally, it is possible that the LV in the CP mouse is exposed to a chronic increase in local and/or systemic sympathetic drive(9, 10, 38, 67), which may also alter gene transcription on the background of that caused by the HIF upregulation itself.

Previous studies of HIF manipulation within the mouse heart have demonstrated an increased reliance upon glucose metabolism, with accompanying contractile dysfunction(7, 24, 35, 40, 41). In the much more modest perturbation of the HIF system in the current study these two features were not coupled, in keeping with a previous study demonstrating that short-term HIF mRNA overexpression could be cardio-protective(32). While there was clear evidence of increased glucose utilization and altered energetics, LV function was enhanced rather than diminished. It is likely that this increased ejection fraction is a reflection of the pulmonary hypertension demonstrated in the CP mice. One potential mechanism is that bowing of the interventricular septum arises as a consequence of the elevated pulmonary arterial pressure, and this could result directly in a reduced LV end-systolic volume. Another possible mechanism is that there is an overall increased sympathetic drive to the heart in order to maintain the

cardiac output in the face of an elevated pulmonary vascular resistance. Again, this would be expected to result in a reduced LV end-systolic volume. It should also be noted that cell types other than cardiomyocytes may be relevant. For example, endothelial cell-specific HIF has been shown to influence cardiac glucose uptake, and this would have effects both *in vivo* and on the isolated perfused-heart preparation (26).

The balance between myocardial glucose and fatty acid metabolism can be studied using the combination of radiolabelled substrates and the isolated perfused-heart(6, 8). We have demonstrated that the hearts from CP mice have elevated glycolytic flux, accompanied by increased net lactate efflux. This finding is in keeping with previous genetic studies which have shown that long-term, constitutive over-expression of HIF-1α in the heart results in increased glucose uptake(24), and that cardiac-specific loss of HIF-1α causes decreased cardiomyocyte lactate concentrations(25). In our study, the increase in glycolytic flux was greater than that of PDH flux, meaning that the decrease in palmitate oxidation did not reach significance. However, following hypoxia, mouse hearts have been shown to have increased glycolytic flux, increased lactate production and significantly decreased fatty acid oxidation (11).

The advent of DNP enables flux through metabolic pathways to be measured in real-time, *in vivo*. This technique has recently been optimized for use in small animals, such as mice, allowing genetic models to be studied for the first time(5, 12). The increased sensitivity (greater than 10, 000-fold(3)) of DNP allows the acquisition of data within one minute after infusion of a bolus of hyperpolarized $^{13}C_1$ pyruvate. This bolus is required to be relatively large, however during the short time-frame of data acquisition no perturbation of plasma metabolites (other than pyruvate) or pyruvate dehydrogenase (PDH) activity occurs(4, 5). Using hyperpolarized $^{13}C_1$ pyruvate MR spectroscopy, we have shown that there is increased rate of label incorporation from pyruvate into both lactate (via LDH) and bicarbonate (via PDH). By using a combination of techniques, we have therefore demonstrated that the measurements of metabolic flux obtained *ex vivo* are in agreement with those made in real-time *in vivo*.

Metabolic flexibility is required for the heart to continue to perform under conditions of varying workload. Inflexibility, due to increased reliance upon a substrate such as glucose (which yields less ATP per molecule, in comparison with fatty acids) may result in myocardial energy depletion. In agreement with this hypothesis, we have demonstrated that myocardial energetics, quantified by measurement of PCr and ATP,

444 are reduced in the CP perfused heart under conditions of increased workload. Altered
445 cardiac energetics are a feature of both heart failure(45) and hypoxia(20, 22, 23); our
446 study adds to this body of evidence by demonstrating that modest long-term
447 upregulation of HIF may result in a similar finding.
448
449 In summary, a modest systemic dysregulation of the HIF pathway, caused by the
450 Chuvash *VHL* mutation, resulted in clear alterations in cardiac metabolism and
451 energetics. However, in contrast to studies generating high levels of HIF in the heart, the
452 CP mice showed neither the predicted changes in gene expression nor any degree of LV
453 impairment. We conclude that the effects of manipulating HIF on the heart are dose-
454 dependent. In the present study, the pulmonary hypertension associated with CP clearly
455 had a significant effect on cardiac function. In future studies employing the CP mutation
456 to study modest HIF dysregulation, targeting this mutation specifically to cardiac
457 myocytes could obviate the influence of pulmonary hypertension.
458

Acknowledgements

We thank Emma Carter and Vicky Ball for expert technical assistance.

Sources of funding

This work was supported by the Wellcome Trust (WT090123AIA, to M.S.), Diabetes UK (11/0004175 to L.C.H.), and by the British Heart Foundation (FS/10/002/28078 to D.T.). Equipment support was provided to D.T. by GE Healthcare, UK.

Disclosures

None

Figure Captions

Figure 1. Cardiac and lung gene expression. Quantitative real-time PCR was used to measure expression of key metabolic genes in hearts from WT (n = 9) and CP (n = 7) mice, aged 6 – 7 months. To confirm the methodology, expression of endothelin 1 (Edn 1; dark gray) was also determined in lungs from thirteen WT and eleven CP mice. Values are mean ± 95% confidence interval. VEGF (vascular endothelial growth factor); GLUT (glucose transporter); PFKM (phosphofructokinase); PDK (pyruvate dehydrogenase kinase); LDHA (lactate dehydrogenase A); PKM (pyruvate kinase muscle); PPARa (peroxisome proliferator-activated receptor α); Edn 1 (endothelin 1). **** ($p < 0.001$).

Figure 2. *In vivo* cardiac function. *In vivo* cine magnetic resonance imaging was used to measure cardiac mass and function in aging WT and CP mice (n = 3 – 8 mice per group). White columns (WT); black columns (CP). (A) Left ventricle (LV) mass; (B) Right ventricle (RV) wall thickness; (C) LV cardiac output, corrected to body mass; (D) LV ejection fraction. WT mice had normal cardiac morphology (E. Representative image of mouse aged 3 – 6 months). CP mice demonstrated marked interventricular septal bowing, particularly in early-diastole (F; arrows. Representative image of mouse aged 3 – 6 months). * ($p < 0.05$); ** ($p < 0.02$); *** ($p < 0.01$).

Figure 3. Perfused-heart energetics. ^{31}P magnetic resonance spectroscopy was performed on perfused hearts from WT and CP mice (n = 5 in each group), aged 6 – 7 months. Body mass 30.1 ± 2.1 g for WT, vs 28.7 ± 1.2 for CP (not significant). White columns (WT); black columns (CP). Hearts were perfused under normal Langendorff conditions using palmitate buffer and spectra were acquired, both without and with an infusion of isoproterenol in order to increase the rate pressure product. As expected, isoproterenol significantly increased the rate pressure product ($p < 0.001$) and decreased the PCR/ATP ratio ($p < 0.001$). No significant difference between WT and CP was detected without isoproterenol, but following the increase in RPP the PCr:ATP ratio was significantly lower in the CP hearts compared with WT controls. (A) rate pressure product; (B) PCr:ATP ratio. ** ($p < 0.02$).

Figure 4. Perfused heart metabolism. Glycolytic flux (A) and net lactate efflux (B) were determined in WT (n = 4) and CP (n = 7) mice, aged 15 – 17 months. Body mass 33.8 ± 1.8 g for WT vs 29.4 ± 1.6 for CP (not significant). Glycolytic and lactate rates were highly correlated (Pearson R = 0.935, $p < 0.001$). Palmitate oxidation rates (C) were determined in separate mice (n = 5 in each group), aged 11 – 17 months. Body mass 27.4 ± 1.5 g for WT vs 26.2 ± 2.0 for CP ($p = 0.034$). *** ($p < 0.01$).

Figure 5. *In vivo* real-time cardiac metabolism. *In vivo* magnetic resonance spectroscopy of hyperpolarized $^{13}C_1$ pyruvate was performed in WT (n = 5) and CP (n = 4) mice, aged 9 – 15 months. Body mass 32.0 ± 3.0 g for WT, vs 27.0 ± 3.0 for CP (not significant). This technique allowed real-time measurement of the rate of label incorporation from pyruvate into alanine (A), bicarbonate (B), or lactate (C). * ($p < 0.05$); *** ($p < 0.01$).

523 **Tables**
524

	Wild type (n)	Chuvash (n)	*p* value
Body mass (male mice, g)	35.9 ± 0.7 (12)	28.4 ± 0.4 (12)	**< 0.001**
Body mass (female mice, g)	25.3 ± 0.3 (4)	23.4 ± 0.5 (8)	**0.016**
Hematocrit (%)	43 ± 0.6 (13)	51 ± 1.0 (13)	**< 0.001**
Hemoglobin (g L^{-1})	138 ± 3 (16)	158 ± 4 (13)	**< 0.001**
Glucose (mmol/L)	13.4 ± 1.0 (7)	13.4 ± 0.5 (7)	0.96
Hydroxybutyrate (mmol/L)	0.18 ± 0.04 (8)	0.21 ± 0.06 (7)	0.65
Non-esterified fatty acid (mmol/L)	0.15 ± 0.01 (8)	0.13 ± 0.02 (7)	0.33
Triacyl glycerol (mmol/L)	2.5 ± 0.2 (7)	2.2 ± 0.5 (7)	0.56
Cholesterol (mmol/L)	1.7 ± 0.20 (8)	1.6 ± 0.05 (7)	0.44

525
526 ***Table 1.*** **Basic hematological and other parameters.** Hematological values, non-
527 fasting plasma metabolites, and body masses of mice aged 6 – 7 months are shown.
528 Results are mean ± SEM; the number of mice used (n) is shown in parentheses.
529

530

		Wild type (n)	Chuvash (n)	*p* value
Body mass (grams)	3 months	28 ± 1.8 (4)	24 ± 1.3 (7)	0.093
	6 months	36 ± 1.1 (4)	25 ± 1.2 (9)	**< 0.0001**
	12 months	37 ± 3.2 (5)	27 ± 0.9 (8)	**0.003**
LV ejection fraction (%)	3 months	61.5 ± 3.7 (3)	71.5 ± 2.2 (6)	**0.043**
	6 months	54.0 ± 1.7 (4)	68.4 ± 3.2 (8)	**0.014**
	12 months	55.5 ± 5.6 (5)	66.5 ± 2.9 (8)	0.078
LV mass (% of body mass)	3 months	0.42 ± 0.01 (3)	0.39 ± 0.02 (6)	0.262
	6 months	0.37 ± 0.04 (5)	0.39 ± 0.01 (7)	0.584
	12 months	0.38 ± 0.04 (5)	0.38 ± 0.02 (8)	0.952
MV RV wall thickness (mm)	3 months	0.35 ± 0.02 (3)	0.47 ± 0.03 (7)	**0.021**
	6 months	0.34 ± 0.02 (5)	0.45 ± 0.02 (8)	**0.001**
	12 months	0.35 ± 0.02 (5)	0.51 ± 0.02 (7)	**0.001**
Septal bowing ratio	3 months	0.91 ± 0.009 (3)	0.83 ± 0.03 (7)	**0.038**
	6 months	0.92 ± 0.004 (5)	0.80 ± 0.01 (7)	**< 0.0001**
	12 months	0.93 ± 0.0 (4)	0.83 ± 0.01 (7)	**< 0.0001**
Heart rate (beats per min)	3 months	420 ± 29 (3)	373 ± 8 (6)	0.069
	6 months	413 ± 10 (5)	398 ± 3 (8)	0.202
	12 months	418 ± 3 (5)	402 ± 7 (8)	0.129
Stroke volume (ml)	3 months	35.1 ± 2.9 (3)	32.2 ± 1.2 (7)	0.282
	6 months	34.5 ± 1.0 (5)	30.8 ± 2.3 (8)	0.24
	12 months	37.1 ± 1.5 (4)	28.1 ± 1.4 (8)	**0.003**
Cardiac output (ml/min)	3 months	14.8 ± 2.0 (3)	12.5 ± 0.8 (7)	0.226
	6 months	14.3 ± 0.5 (5)	12.2 ± 0.9 (8)	0.116
	12 months	14.6 ± 1.2 (5)	11.3 ± 0.7 (8)	**0.025**
LV Cardiac index (ml/min/g)	3 months	0.54 ± 0.03 (3)	0.52 ± 0.03 (7)	0.756
	6 months	0.43 ± 0.03 (5)	0.48 ± 0.03 (8)	0.197
	12 months	0.40 ± 0.01 (5)	0.43 ± 0.02 (8)	0.322

531
532 ***Table 2.*** **Full cine MRI data.** Results are mean ± SEM; the number of mice used (n) is
533 shown in parentheses. For the 'Septal bowing ratio', the greater the distortion of the LV
534 by the septum, the greater the deviation from the perfect circle ratio of 1.0.
535

References

1. **Adrogue JV, Sharma S, Ngumbela K, Essop MF, and Taegtmeyer H**. Acclimatization to chronic hypobaric hypoxia is associated with a differential transcriptional profile between the right and left ventricle. *Molecular and cellular biochemistry* 278: 71-78, 2005.
2. **Ang SO, Chen H, Hirota K, Gordeuk VR, Jelinek J, Guan Y, Liu E, Sergueeva AI, Miasnikova GY, Mole D, Maxwell PH, Stockton DW, Semenza GL, and Prchal JT**. Disruption of oxygen homeostasis underlies congenital Chuvash polycythemia. *Nature genetics* 32: 614-621, 2002.
3. **Ardenkjaer-Larsen JH, Fridlund B, Gram A, Hansson G, Hansson L, Lerche MH, Servin R, Thaning M, and Golman K**. Increase in signal-to-noise ratio of > 10,000 times in liquid-state NMR. *Proceedings of the National Academy of Sciences of the United States of America* 100: 10158-10163, 2003.
4. **Atherton HJ, Schroeder MA, Dodd MS, Heather LC, Carter EE, Cochlin LE, Nagel S, Sibson NR, Radda GK, Clarke K, and Tyler DJ**. Validation of the in vivo assessment of pyruvate dehydrogenase activity using hyperpolarised 13C MRS. *NMR in biomedicine* 24: 201-208, 2011.
5. **Bakermans AJ, Dodd MS, Nicolay K, Prompers JJ, Tyler DJ, and Houten SM**. Myocardial energy shortage and unmet anaplerotic needs in the fasted long-chain acyl-CoA dehydrogenase knockout mouse. *Cardiovascular research* 100: 441-449, 2013.
6. **Barr RL, and Lopaschuk GD**. Direct measurement of energy metabolism in the isolated working rat heart. *Journal of pharmacological and toxicological methods* 38: 11-17, 1997.
7. **Bekeredjian R, Walton CB, MacCannell KA, Ecker J, Kruse F, Outten JT, Sutcliffe D, Gerard RD, Bruick RK, and Shohet RV**. Conditional HIF-1alpha expression produces a reversible cardiomyopathy. *PloS one* 5: e11693, 2010.
8. **Belke DD, Larsen TS, Lopaschuk GD, and Severson DL**. Glucose and fatty acid metabolism in the isolated working mouse heart. *The American journal of physiology* 277: R1210-1217, 1999.
9. **Ciarka A, Doan V, Velez-Roa S, Naeije R, and van de Borne P**. Prognostic significance of sympathetic nervous system activation in pulmonary arterial hypertension. *American journal of respiratory and critical care medicine* 181: 1269-1275, 2010.
10. **Ciarka A, Vachiery JL, Houssiere A, Gujic M, Stoupel E, Velez-Roa S, Naeije R, and van de Borne P**. Atrial septostomy decreases sympathetic overactivity in pulmonary arterial hypertension. *Chest* 131: 1831-1837, 2007.
11. **Cole MA, Abd Jamil AH, Heather LC, Murray AJ, Sutton ER, Slingo M, Sebag-Montefiore L, Tan SC, Aksentijevic D, Gildea OS, Stuckey DJ, Yeoh KK, Carr CA, Evans RD, Aasum E, Schofield CJ, Ratcliffe PJ, Neubauer S, Robbins PA, and Clarke K**. On the pivotal role of PPARalpha in adaptation of the heart to hypoxia and why fat in the diet increases hypoxic injury. *FASEB journal : official publication of the Federation of American Societies for Experimental Biology* 2016.
12. **Dodd MS, Ball V, Bray R, Ashrafian H, Watkins H, Clarke K, and Tyler DJ**. In vivo mouse cardiac hyperpolarized magnetic resonance spectroscopy. *Journal of cardiovascular magnetic resonance : official journal of the Society for Cardiovascular Magnetic Resonance* 15: 19, 2013.

13. **Formenti F, Beer PA, Croft QP, Dorrington KL, Gale DP, Lappin TR, Lucas GS, Maher ER, Maxwell PH, McMullin MF, O'Connor DF, Percy MJ, Pugh CW, Ratcliffe PJ, Smith TG, Talbot NP, and Robbins PA**. Cardiopulmonary function in two human disorders of the hypoxia-inducible factor (HIF) pathway: von Hippel-Lindau disease and HIF-2alpha gain-of-function mutation. *FASEB journal : official publication of the Federation of American Societies for Experimental Biology* 25: 2001-2011, 2011.

14. **Formenti F, Constantin-Teodosiu D, Emmanuel Y, Cheeseman J, Dorrington KL, Edwards LM, Humphreys SM, Lappin TR, McMullin MF, McNamara CJ, Mills W, Murphy JA, O'Connor DF, Percy MJ, Ratcliffe PJ, Smith TG, Treacy M, Frayn KN, Greenhaff PL, Karpe F, Clarke K, and Robbins PA**. Regulation of human metabolism by hypoxia-inducible factor. *Proceedings of the National Academy of Sciences of the United States of America* 107: 12722-12727, 2010.

15. **Gordeuk VR, Miasnikova GY, Sergueeva AI, Niu X, Nouraie M, Okhotin DJ, Polyakova LA, Ammosova T, Nekhai S, Ganz T, and Prchal JT**. Chuvash polycythemia VHLR200W mutation is associated with down-regulation of hepcidin expression. *Blood* 118: 5278-5282, 2011.

16. **Gordeuk VR, Sergueeva AI, Miasnikova GY, Okhotin D, Voloshin Y, Choyke PL, Butman JA, Jedlickova K, Prchal JT, and Polyakova LA**. Congenital disorder of oxygen sensing: association of the homozygous Chuvash polycythemia VHL mutation with thrombosis and vascular abnormalities but not tumors. *Blood* 103: 3924-3932, 2004.

17. **Heather LC, Cole MA, Tan JJ, Ambrose LJ, Pope S, Abd-Jamil AH, Carter EE, Dodd MS, Yeoh KK, Schofield CJ, and Clarke K**. Metabolic adaptation to chronic hypoxia in cardiac mitochondria. *Basic research in cardiology* 107: 268, 2012.

18. **Hickey MM, Lam JC, Bezman NA, Rathmell WK, and Simon MC**. von Hippel-Lindau mutation in mice recapitulates Chuvash polycythemia via hypoxia-inducible factor-2alpha signaling and splenic erythropoiesis. *The Journal of clinical investigation* 117: 3879-3889, 2007.

19. **Hickey MM, Richardson T, Wang T, Mosqueira M, Arguiri E, Yu H, Yu QC, Solomides CC, Morrisey EE, Khurana TS, Christofidou-Solomidou M, and Simon MC**. The von Hippel-Lindau Chuvash mutation promotes pulmonary hypertension and fibrosis in mice. *The Journal of clinical investigation* 120: 827-839, 2010.

20. **Hochachka PW, Clark CM, Holden JE, Stanley C, Ugurbil K, and Menon RS**. 31P magnetic resonance spectroscopy of the Sherpa heart: a phosphocreatine/adenosine triphosphate signature of metabolic defense against hypobaric hypoxia. *Proceedings of the National Academy of Sciences of the United States of America* 93: 1215-1220, 1996.

21. **Holden JE, Stone CK, Clark CM, Brown WD, Nickles RJ, Stanley C, and Hochachka PW**. Enhanced cardiac metabolism of plasma glucose in high-altitude natives: adaptation against chronic hypoxia. *Journal of applied physiology* 79: 222-228, 1995.

22. **Holloway C, Cochlin L, Codreanu I, Bloch E, Fatemian M, Szmigielski C, Atherton H, Heather L, Francis J, Neubauer S, Robbins P, Montgomery H, and Clarke K**. Normobaric hypoxia impairs human cardiac energetics. *FASEB*

journal : official publication of the Federation of American Societies for Experimental Biology 25: 3130-3135, 2011.

23. **Holloway CJ, Montgomery HE, Murray AJ, Cochlin LE, Codreanu I, Hopwood N, Johnson AW, Rider OJ, Levett DZ, Tyler DJ, Francis JM, Neubauer S, Grocott MP, Clarke K, and Caudwell Xtreme Everest Research G**. Cardiac response to hypobaric hypoxia: persistent changes in cardiac mass, function, and energy metabolism after a trek to Mt. Everest Base Camp. *FASEB journal : official publication of the Federation of American Societies for Experimental Biology* 25: 792-796, 2011.

24. **Holscher M, Schafer K, Krull S, Farhat K, Hesse A, Silter M, Lin Y, Pichler BJ, Thistlethwaite P, El-Armouche A, Maier LS, Katschinski DM, and Zieseniss A**. Unfavourable consequences of chronic cardiac HIF-1alpha stabilization. *Cardiovascular research* 94: 77-86, 2012.

25. **Huang Y, Hickey RP, Yeh JL, Liu D, Dadak A, Young LH, Johnson RS, and Giordano FJ**. Cardiac myocyte-specific HIF-1alpha deletion alters vascularization, energy availability, calcium flux, and contractility in the normoxic heart. *FASEB journal : official publication of the Federation of American Societies for Experimental Biology* 18: 1138-1140, 2004.

26. **Huang Y, Lei L, Liu D, Jovin I, Russell R, Johnson RS, Di Lorenzo A, and Giordano FJ**. Normal glucose uptake in the brain and heart requires an endothelial cell-specific HIF-1alpha-dependent function. *Proceedings of the National Academy of Sciences of the United States of America* 109: 17478-17483, 2012.

27. **Hue L, and Taegtmeyer H**. The Randle cycle revisited: a new head for an old hat. *American journal of physiology Endocrinology and metabolism* 297: E578-591, 2009.

28. **Hurford WE, Crosby G, Strauss HW, Jones R, and Lowenstein E**. Ventricular performance and glucose uptake in rats during chronic hypobaric hypoxia. *Journal of nuclear medicine : official publication, Society of Nuclear Medicine* 31: 1344-1351, 1990.

29. **Hyvarinen J, Hassinen IE, Sormunen R, Maki JM, Kivirikko KI, Koivunen P, and Myllyharju J**. Hearts of hypoxia-inducible factor prolyl 4-hydroxylase-2 hypomorphic mice show protection against acute ischemia-reperfusion injury. *The Journal of biological chemistry* 285: 13646-13657, 2010.

30. **Iyer NV, Kotch LE, Agani F, Leung SW, Laughner E, Wenger RH, Gassmann M, Gearhart JD, Lawler AM, Yu AY, and Semenza GL**. Cellular and developmental control of O2 homeostasis by hypoxia-inducible factor 1 alpha. *Genes & development* 12: 149-162, 1998.

31. **Kaelin WG, Jr., and Ratcliffe PJ**. Oxygen sensing by metazoans: the central role of the HIF hydroxylase pathway. *Molecular cell* 30: 393-402, 2008.

32. **Kido M, Du L, Sullivan CC, Li X, Deutsch R, Jamieson SW, and Thistlethwaite PA**. Hypoxia-inducible factor 1-alpha reduces infarction and attenuates progression of cardiac dysfunction after myocardial infarction in the mouse. *Journal of the American College of Cardiology* 46: 2116-2124, 2005.

33. **Kim JW, Tchernyshyov I, Semenza GL, and Dang CV**. HIF-1-mediated expression of pyruvate dehydrogenase kinase: a metabolic switch required for cellular adaptation to hypoxia. *Cell metabolism* 3: 177-185, 2006.

34. **Lamb HJ, Beyerbacht HP, van der Laarse A, Stoel BC, Doornbos J, van der Wall EE, and de Roos A**. Diastolic Dysfunction in Hypertensive Heart

Disease Is Associated With Altered Myocardial Metabolism. *Circulation* 99: 2261-2267, 1999.

35. **Lei L, Mason S, Liu D, Huang Y, Marks C, Hickey R, Jovin IS, Pypaert M, Johnson RS, and Giordano FJ**. Hypoxia-inducible factor-dependent degeneration, failure, and malignant transformation of the heart in the absence of the von Hippel-Lindau protein. *Molecular and cellular biology* 28: 3790-3803, 2008.

36. **Loenarz C, Coleman ML, Boleininger A, Schierwater B, Holland PW, Ratcliffe PJ, and Schofield CJ**. The hypoxia-inducible transcription factor pathway regulates oxygen sensing in the simplest animal, Trichoplax adhaerens. *EMBO reports* 12: 63-70, 2011.

37. **Lorenzo FR, Yang C, Ng Tang Fui M, Vankayalapati H, Zhuang Z, Huynh T, Grossmann M, Pacak K, and Prchal JT**. A novel EPAS1/HIF2A germline mutation in a congenital polycythemia with paraganglioma. *Journal of molecular medicine* 91: 507-512, 2013.

38. **Mak S, Witte KK, Al-Hesayen A, Granton JJ, and Parker JD**. Cardiac sympathetic activation in patients with pulmonary arterial hypertension. *American journal of physiology Regulatory, integrative and comparative physiology* 302: R1153-1157, 2012.

39. **McClain DA, Abuelgasim KA, Nouraie M, Salomon-Andonie J, Niu X, Miasnikova G, Polyakova LA, Sergueeva A, Okhotin DJ, Cherqaoui R, Okhotin D, Cox JE, Swierczek S, Song J, Simon MC, Huang J, Simcox JA, Yoon D, Prchal JT, and Gordeuk VR**. Decreased serum glucose and glycosylated hemoglobin levels in patients with Chuvash polycythemia: a role for HIF in glucose metabolism. *Journal of molecular medicine* 91: 59-67, 2013.

40. **Minamishima YA, Moslehi J, Bardeesy N, Cullen D, Bronson RT, and Kaelin WG, Jr.** Somatic inactivation of the PHD2 prolyl hydroxylase causes polycythemia and congestive heart failure. *Blood* 111: 3236-3244, 2008.

41. **Moslehi J, Minamishima YA, Shi J, Neuberg D, Charytan DM, Padera RF, Signoretti S, Liao R, and Kaelin WG, Jr.** Loss of hypoxia-inducible factor prolyl hydroxylase activity in cardiomyocytes phenocopies ischemic cardiomyopathy. *Circulation* 122: 1004-1016, 2010.

42. **Naressi A, Couturier C, Castang I, de Beer R, and Graveron-Demilly D**. Java-based graphical user interface for MRUI, a software package for quantitation of in vivo/medical magnetic resonance spectroscopy signals. *Computers in biology and medicine* 31: 269-286, 2001.

43. **Neubauer S**. The failing heart--an engine out of fuel. *The New England journal of medicine* 356: 1140-1151, 2007.

44. **Neubauer S, Horn M, Cramer M, Harre K, Newell JB, Peters W, Pabst T, Ertl G, Hahn D, Ingwall JS, and Kochsiek K**. Myocardial phosphocreatine-to-ATP ratio is a predictor of mortality in patients with dilated cardiomyopathy. *Circulation* 96: 2190-2196, 1997.

45. **Neubauer S, Horn M, Pabst T, Godde M, Lubke D, Jilling B, Hahn D, and Ertl G**. Contributions of 31P-magnetic resonance spectroscopy to the understanding of dilated heart muscle disease. *European heart journal* 16 Suppl O: 115-118, 1995.

46. **Niu X, Miasnikova GY, Sergueeva AI, Polyakova LA, Okhotin DJ, Tuktanov NV, Nouraie M, Ammosova T, Nekhai S, and Gordeuk VR**. Altered

729 cytokine profiles in patients with Chuvash polycythemia. *American journal of*
730 *hematology* 84: 74-78, 2009.
731 47. **Papandreou I, Cairns RA, Fontana L, Lim AL, and Denko NC**. HIF-1
732 mediates adaptation to hypoxia by actively downregulating mitochondrial
733 oxygen consumption. *Cell metabolism* 3: 187-197, 2006.
734 48. **Pastore YD, Jelinek J, Ang S, Guan Y, Liu E, Jedlickova K, Krishnamurti**
735 **L, and Prchal JT**. Mutations in the VHL gene in sporadic apparently congenital
736 polycythemia. *Blood* 101: 1591-1595, 2003.
737 49. **Paul SA, Simons JW, and Mabjeesh NJ**. HIF at the crossroads between
738 ischemia and carcinogenesis. *Journal of cellular physiology* 200: 20-30, 2004.
739 50. **Percy MJ**. Familial erythrocytosis arising from a gain-of-function
740 mutation in the HIF2A gene of the oxygen sensing pathway. *The Ulster medical*
741 *journal* 77: 86-88, 2008.
742 51. **Percy MJ, McMullin MF, Jowitt SN, Potter M, Treacy M, Watson WH,**
743 **and Lappin TR**. Chuvash-type congenital polycythemia in 4 families of Asian and
744 Western European ancestry. *Blood* 102: 1097-1099, 2003.
745 52. **Perrotta S, Nobili B, Ferraro M, Migliaccio C, Borriello A, Cucciolla V,**
746 **Martinelli V, Rossi F, Punzo F, Cirillo P, Parisi G, Zappia V, Rotoli B, and**
747 **Della Ragione F**. Von Hippel-Lindau-dependent polycythemia is endemic on the
748 island of Ischia: identification of a novel cluster. *Blood* 107: 514-519, 2006.
749 53. **Perrotta S, Stiehl DP, Punzo F, Scianguetta S, Borriello A, Bencivenga**
750 **D, Casale M, Nobili B, Fasoli S, Balduzzi A, Cro L, Nytko KJ, Wenger RH, and**
751 **Della Ragione F**. Congenital erythrocytosis associated with gain-of-function
752 HIF2A gene mutations and erythropoietin levels in the normal range.
753 *Haematologica* 98: 1624-1632, 2013.
754 54. **Prabhakar NR, and Semenza GL**. Adaptive and maladaptive
755 cardiorespiratory responses to continuous and intermittent hypoxia mediated
756 by hypoxia-inducible factors 1 and 2. *Physiological reviews* 92: 967-1003, 2012.
757 55. **Razeghi P, Young ME, Abbasi S, and Taegtmeyer H**. Hypoxia in vivo
758 decreases peroxisome proliferator-activated receptor alpha-regulated gene
759 expression in rat heart. *Biochemical and biophysical research communications*
760 287: 5-10, 2001.
761 56. **Ryan T, Petrovic O, Dillon JC, Feigenbaum H, Conley MJ, and**
762 **Armstrong WF**. An echocardiographic index for separation of right ventricular
763 volume and pressure overload. *Journal of the American College of Cardiology* 5:
764 918-927, 1985.
765 57. **Sable CA, Aliyu ZY, Dham N, Nouraie M, Sachdev V, Sidenko S,**
766 **Miasnikova GY, Polyakova LA, Sergueeva AI, Okhotin DJ, Bushuev V,**
767 **Remaley AT, Niu X, Castro OL, Gladwin MT, Kato GJ, Prchal JT, and Gordeuk**
768 **VR**. Pulmonary artery pressure and iron deficiency in patients with upregulation
769 of hypoxia sensing due to homozygous VHL(R200W) mutation (Chuvash
770 polycythemia). *Haematologica* 97: 193-200, 2012.
771 58. **Schneider JE, Cassidy PJ, Lygate C, Tyler DJ, Wiesmann F, Grieve SM,**
772 **Hulbert K, Clarke K, and Neubauer S**. Fast, high-resolution in vivo cine
773 magnetic resonance imaging in normal and failing mouse hearts on a vertical
774 11.7 T system. *Journal of magnetic resonance imaging : JMRI* 18: 691-701, 2003.
775 59. **Schroeder MA, Atherton HJ, Ball DR, Cole MA, Heather LC, Griffin JL,**
776 **Clarke K, Radda GK, and Tyler DJ**. Real-time assessment of Krebs cycle
777 metabolism using hyperpolarized 13C magnetic resonance spectroscopy. *FASEB*

journal : official publication of the Federation of American Societies for Experimental Biology 23: 2529-2538, 2009.

60. **Seagroves TN, Ryan HE, Lu H, Wouters BG, Knapp M, Thibault P, Laderoute K, and Johnson RS**. Transcription factor HIF-1 is a necessary mediator of the pasteur effect in mammalian cells. *Molecular and cellular biology* 21: 3436-3444, 2001.

61. **Semenza GL, Jiang BH, Leung SW, Passantino R, Concordet JP, Maire P, and Giallongo A**. Hypoxia response elements in the aldolase A, enolase 1, and lactate dehydrogenase A gene promoters contain essential binding sites for hypoxia-inducible factor 1. *The Journal of biological chemistry* 271: 32529-32537, 1996.

62. **Sharma S, Taegtmeyer H, Adrogue J, Razeghi P, Sen S, Ngumbela K, and Essop MF**. Dynamic changes of gene expression in hypoxia-induced right ventricular hypertrophy. *American journal of physiology Heart and circulatory physiology* 286: H1185-1192, 2004.

63. **Sivitz WI, Lund DD, Yorek B, Grover-McKay M, and Schmid PG**. Pretranslational regulation of two cardiac glucose transporters in rats exposed to hypobaric hypoxia. *The American journal of physiology* 263: E562-569, 1992.

64. **Slingo ME, Turner PJ, Christian HC, Buckler KJ, and Robbins PA**. The von Hippel-Lindau Chuvash mutation in mice causes carotid-body hyperplasia and enhanced ventilatory sensitivity to hypoxia. *Journal of applied physiology* 116: 885-892, 2014.

65. **Smith TG, Brooks JT, Balanos GM, Lappin TR, Layton DM, Leedham DL, Liu C, Maxwell PH, McMullin MF, McNamara CJ, Percy MJ, Pugh CW, Ratcliffe PJ, Talbot NP, Treacy M, and Robbins PA**. Mutation of von Hippel-Lindau tumour suppressor and human cardiopulmonary physiology. *PLoS medicine* 3: e290, 2006.

66. **Tan Q, Kerestes H, Percy MJ, Pietrofesa R, Chen L, Khurana TS, Christofidou-Solomidou M, Lappin TR, and Lee FS**. Erythrocytosis and pulmonary hypertension in a mouse model of human HIF2A gain of function mutation. *The Journal of biological chemistry* 288: 17134-17144, 2013.

67. **Velez-Roa S, Ciarka A, Najem B, Vachiery JL, Naeije R, and van de Borne P**. Increased sympathetic nerve activity in pulmonary artery hypertension. *Circulation* 110: 1308-1312, 2004.

68. **Yang C, Sun MG, Matro J, Huynh TT, Rahimpour S, Prchal JT, Lechan R, Lonser R, Pacak K, and Zhuang Z**. Novel HIF2A mutations disrupt oxygen sensing, leading to polycythemia, paragangliomas, and somatostatinomas. *Blood* 121: 2563-2566, 2013.

69. **Yoon D, Okhotin DV, Kim B, Okhotina Y, Okhotin DJ, Miasnikova GY, Sergueeva AI, Polyakova LA, Maslow A, Lee Y, Semenza GL, Prchal JT, and Gordeuk VR**. Increased size of solid organs in patients with Chuvash polycythemia and in mice with altered expression of HIF-1alpha and HIF-2alpha. *Journal of molecular medicine* 88: 523-530, 2010.

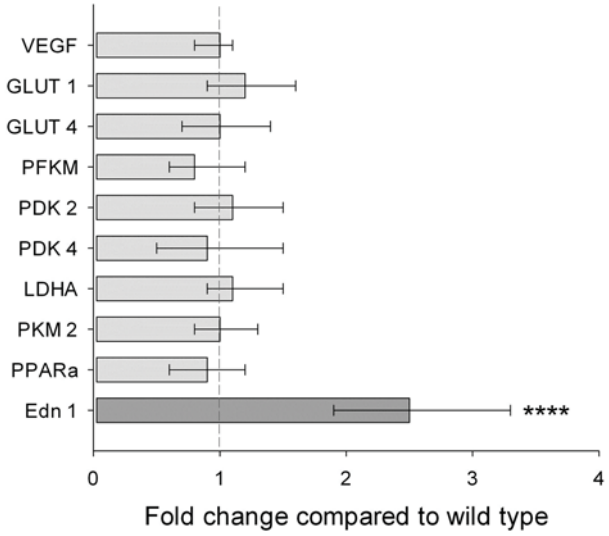
VEGF
GLUT 1
GLUT 4
PFKM
PDK 2
PDK 4
LDHA
PKM 2
PPARa
Edn 1
****
0
1
2
3
4
Fold change compared to wild type

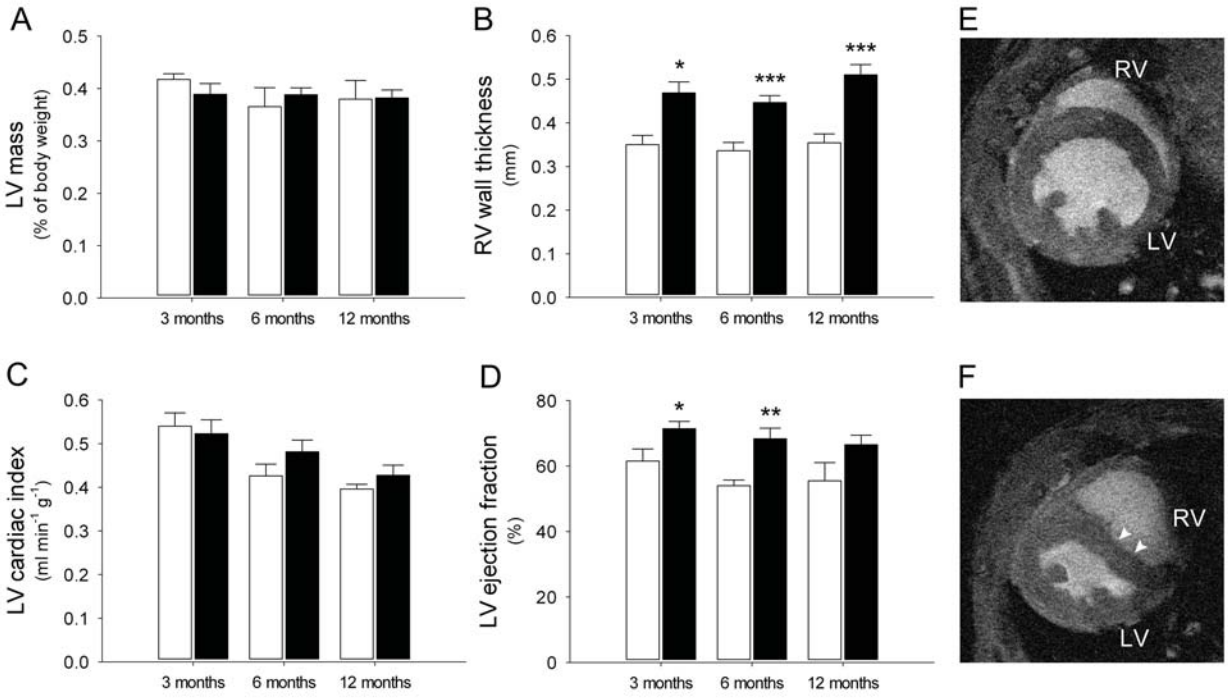
A
LV mass
(% of body weight)
0.5
0.4
0.3
0.2
0.1
0.0
3 months
6 months
12 months
B
RV wall thickness
(mm)
0.6
0.5
0.4
0.3
0.2
0.1
0.0
*
***
***
3 months
6 months
12 months
E
RV
LV
C
LV cardiac index
(ml min-1 g-1)
0.6
0.5
0.4
0.3
0.2
0.1
0.0
3 months
6 months
12 months
D
LV ejection fraction
(%)
80
60
40
20
0
*
**
3 months
6 months
12 months
F
RV
LV

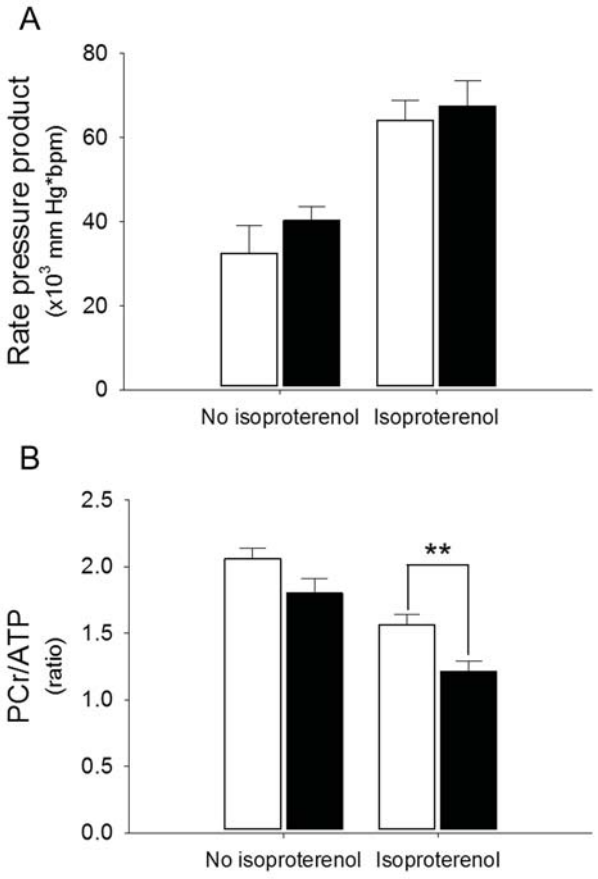
A
Rate pressure product
(x10^3 mm Hg*bpm)
80
60
40
20
0
No isoproterenol
Isoproterenol
B
PCr/ATP
(ratio)
2.5
2.0
1.5
1.0
0.5
0.0
**
No isoproterenol
Isoproterenol

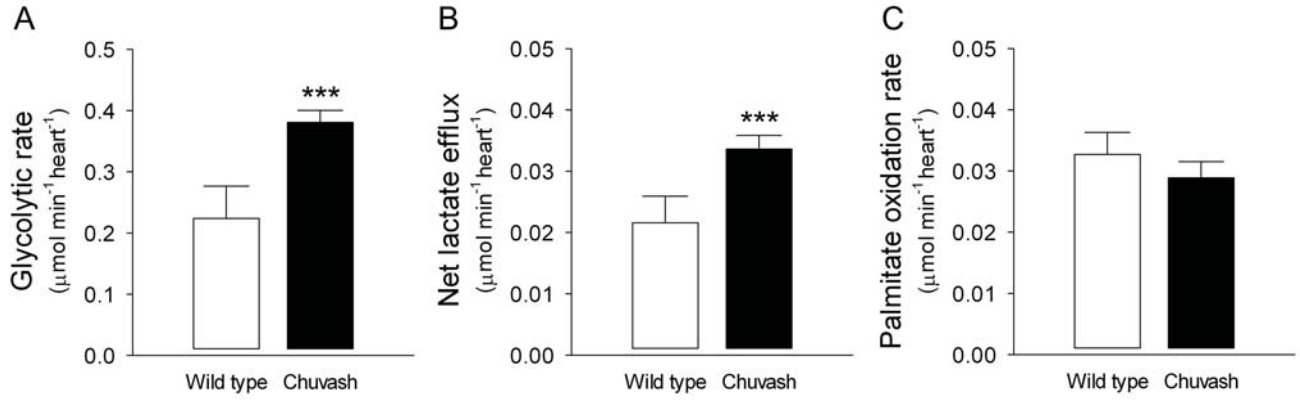
A
Glycolytic rate
(μmol min-1 heart-1)
0.5
0.4
0.3
0.2
0.1
0.0
***
Wild type
Chuvash
B
Net lactate efflux
(μmol min-1 heart-1)
0.05
0.04
0.03
0.02
0.01
0.00
***
Wild type
Chuvash
C
Palmitate oxidation rate
(μmol min-1 heart-1)
0.05
0.04
0.03
0.02
0.01
0.00
Wild type
Chuvash

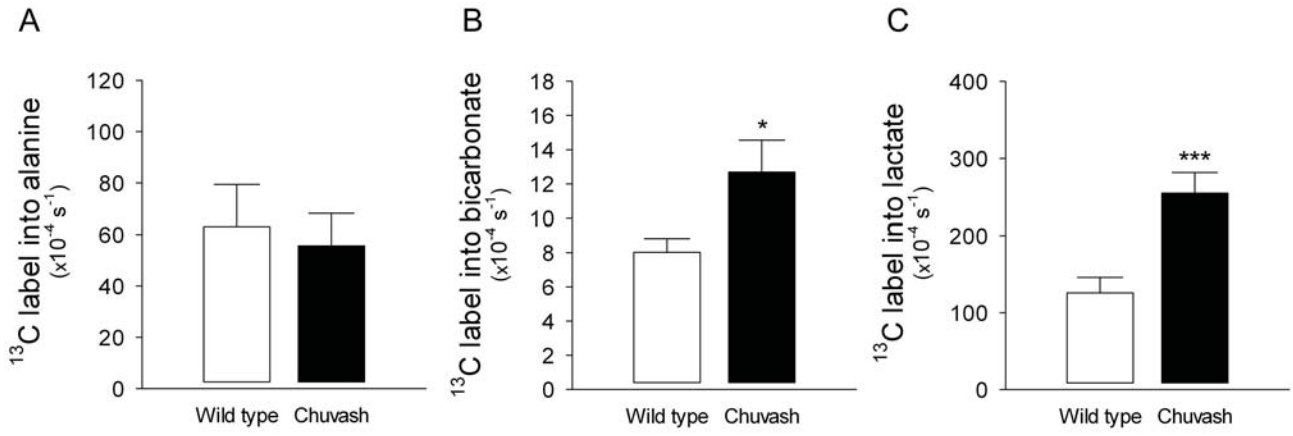
A
^{13}C label into alanine
(x10^{-4} s^{-1})
120
100
80
60
40
20
0
Wild type
Chuvash
B
^{13}C label into bicarbonate
(x10^{-4} s^{-1})
18
16
14
12
10
8
6
4
2
0
*
Wild type
Chuvash
C
^{13}C label into lactate
(x10^{-4} s^{-1})
400
300
200
100
0
***
Wild type
Chuvash